AMERICAN SOCIETY FOR MICROBIOLOGY | Molecular and Cellular Biology®

RESEARCH ARTICLE

Infertility Caused by Inefficient Apoptotic Germ Cell Clearance in *Xkr8*-Deficient Male Mice

Yahiro Yamashita,[a] Chigure Suzuki,[b,c] Yasuo Uchiyama,[b] Shigekazu Nagata[a]

[a]Laboratory of Biochemistry & Immunology, World Premier International Research Center, Immunology Frontier Research Center, Osaka University, Osaka, Japan
[b]Department of Cellular and Molecular Neuropathology, Juntendo University Graduate School of Medicine, Tokyo, Japan
[c]Department of Cellular and Molecular Pharmacology, Juntendo University Graduate School of Medicine, Tokyo, Japan

ABSTRACT During spermatogenesis, up to 75% of germ cells in the testes undergo apoptosis and are cleared by Sertoli cells. X-linked XK blood group-related 8 (Xkr8) is a plasma membrane protein that scrambles phospholipids in response to apoptotic signals, exposing phosphatidylserine (PtdSer). Here, we found that *Xkr8*$^{-/-}$ male mice were infertile due to reduced sperm counts in their epididymides. Apoptotic stimuli could not induce PtdSer exposure in *Xkr8*$^{-/-}$ germ cells. Consistent with the hypothesis that PtdSer functions as an "eat-me" signal to phagocytes, cells expressing phosphatidylserine receptor TIM4 and MER tyrosine kinase receptor efficiently engulfed apoptotic wild-type male germ cells but not *Xkr8*$^{-/-}$ germ cells. Fluorescence and electron microscopy revealed Sertoli cells carrying engulfed and degenerated dead cells. However, many unengulfed apoptotic cells and residual bodies and much cell debris were present in *Xkr8*$^{-/-}$ testes and epididymides. These results indicate that Xkr8-mediated PtdSer exposure is essential for the clearance of apoptotic germ cells by Sertoli cells. There was no apparent inflammation in *Xkr8*$^{-/-}$ testes, suggesting that the unengulfed apoptotic cells may have undergone secondary necrosis, releasing noxious materials that affected the germ cells. Alternatively, failure to engulf the apoptotic germ cells may have caused the Sertoli cells to starve and lose their ability to support spermatogenesis.

KEYWORDS apoptosis, phospholipid scramblase, spermatogenesis, Sertoli cells, male infertility, Xkr8

During animal tissue development, many useless or harmful cells are generated which eventually undergo apoptosis (1). In our daily life, cells infected by viruses or bacteria may die via pyroptosis or necroptosis (2), but starved cells and cells damaged by DNA-damaging agents die via apoptosis. Cytotoxic lymphocytes (CTL) and natural killer (NK) cells kill target cells by inducing apoptosis (3).

Apoptosis is mediated by two pathways (4, 5). The intrinsic pathway is triggered by DNA-damaging agents, factor deprivation, or programmed transcriptional activation of the death-inducing system during animal development. The extrinsic pathway is triggered by external death factors such as tumor necrosis factor (TNF), Fas ligand (FasL), and TNF-related apoptosis-inducing ligand, all of which are expressed on the surface of CTL and NK cells. The intrinsic death pathway activates the caspase cascade via the sequential activation of BH3-only proteins, translocation of BAX and BAK to the mitochondria, cytochrome *c* release from mitochondria, and caspase 9 activation. In the extrinsic pathway, death factors bind to death receptors and activate caspase 8 through the oligomerization of Fas-associated protein with death domain (FADD). Both pathways result in the activation of caspase 3, an executioner caspase that cleaves nearly 1,300 substrates (6), inducing the general characteristics of apoptosis, including DNA fragmentation, membrane blebbing, and phosphatidylserine (PtdSer) exposure (7).

Citation Yamashita Y, Suzuki C, Uchiyama Y, Nagata S. 2020. Infertility caused by inefficient apoptotic germ cell clearance in *Xkr8*-deficient male mice. Mol Cell Biol 40:e00402-19. https://doi.org/10.1128/MCB.00402-19.

Address correspondence to Shigekazu Nagata, snagata@ifrec.osaka-u.ac.jp.

Received 27 August 2019
Returned for modification 30 September 2019
Accepted 4 November 2019
Accepted manuscript posted online 11 November 2019
Published 16 January 2020

Apoptotic cells are efficiently eliminated by phagocytes to prevent the release of noxious materials (8, 9). Phagocytes engulf apoptotic cells by recognizing PtdSer, which serves as an "eat-me" signal (8). In living cells, PtdSer exists in the inner leaflet of the plasma membrane but is exposed to the cell surface during apoptosis (10–12). We previously showed that X-linked XK blood group-related 8 (Xkr8), a membrane protein with 10 putative transmembrane segments, is cleaved by caspase 3 at its C-terminal tail region and functions as a phospholipid scramblase, destroying the asymmetrical distribution of phospholipids at the plasma membrane and exposing PtdSer (13). Caspase 3 also cleaves and inactivates the type IV-P-type ATPases, namely, ATP11A and ATP11C, which are flippases that specifically translocate PtdSer from the outer leaflet of the plasma membrane to the inner leaflet (14, 15). Thus, the PtdSer exposed by the scramblase activity of Xkr8 in apoptotic cells cannot return to the inner leaflet and irreversibly remains on the surface as an eat-me signal for phagocytes.

During spermatogenesis, 75% of germ cells undergo apoptosis at various stages and are cleared by Sertoli cells in the testes (16–19). We therefore examined the effects of *Xkr8* knockout on spermatogenesis. In contrast to wild-type testes, which increased in weight until 15 weeks of age, the testicular weights of *Xkr8*$^{-/-}$ males increased only until 5 weeks of age, and their sperm counts at 14 to 17 weeks of age were less than 25% of those of wild-type males. *Xkr8*-deficient male mice are infertile, and of the three Xkr family members (Xkr4, Xkr8, and Xkr9) that function as caspase-dependent scramblases (20), only Xkr8 is expressed in male germ cells. Treatment of *Xkr8*$^{-/-}$ male germ cells with a BH3-mimetic activated caspase 3 but did not induce PtdSer exposure. Sertoli cells in wild-type testes were observed carrying apoptotic cells, but most of the apoptotic cells in *Xkr8*$^{-/-}$ testes were outside Sertoli cells. The results indicate that PtdSer-dependent engulfment of apoptotic germ cells during first-round spermatogenesis is essential for productive spermatogenesis.

RESULTS

Testicular dysgenesis in *Xkr8*$^{-/-}$ males. We previously established *Xkr8*-deficient mice in the C57BL/6 background (13); the mice grew normally and had no apparent abnormalities in appearance or behavior. However, although intercrossing *Xkr8*$^{+/-}$ mice produced offspring as productively as wild-type B6 mice, intercrossing *Xkr8*$^{-/-}$ mice produced almost no offspring. As shown in Fig. 1A, when 8- to 12-week-old *Xkr8*$^{-/-}$ female mice were crossed with wild-type B6 males, the number of offspring was similar to the numbers obtained with *Xkr8*$^{+/+}$ or *Xkr8*$^{+/-}$ female mice. Conversely, when 10- to 12-week-old *Xkr8*$^{-/-}$ male mice were crossed with 9-week-old wild-type female ICR mice, which are known to be prolific (21, 22), they generated no offspring in 10/12 challenges (Fig. 1A). In two cases, *Xkr8*$^{-/-}$ mice produced offspring, but the litters contained only two and six pups, respectively. The average number of offspring obtained with *Xkr8*$^{-/-}$ males was extremely low (0.7) compared with the average number of offspring obtained with *Xkr8*$^{+/-}$ males (12.6).

Since the testes of 10-week-old *Xkr8*-null mice were significantly smaller than those of wild-type mice, we examined their weights. Consistent with previous reports (23, 24), the testicular weights of wild-type mice increased approximately 11-fold from 2 to 15 weeks of age (Fig. 1B). As expected, since there was little difference in fertility between *Xkr8*$^{+/+}$ and *Xkr8*$^{+/-}$ male mice, the weights of their testes were comparable. The weights of *Xkr8*$^{-/-}$ testes increased similarly until 5 weeks of age but increased little in subsequent weeks (Fig. 1B). The increase in testicular weight is due to the spermatogenesis that occurs after birth. Accordingly, sperm counts in the cauda epididymides of 14- to 17-week-old *Xkr8*$^{-/-}$ mice were approximately 25% of those observed in *Xkr8*$^{+/-}$ mice (Fig. 1C), but their morphology was similar to that of the Xkr8$^{+/-}$ sperm (Fig. 1D).

Histological analysis indicated that the seminiferous tubules of *Xkr8*$^{-/-}$ testes were abnormal, containing aggregated cells and Sertoli cells with many vacuoles (Fig. 1E). The number of germ cells was significantly reduced by *Xkr8* knockout in a portion of seminiferous tubules. This testicular abnormality was more pronounced in 30-week-old

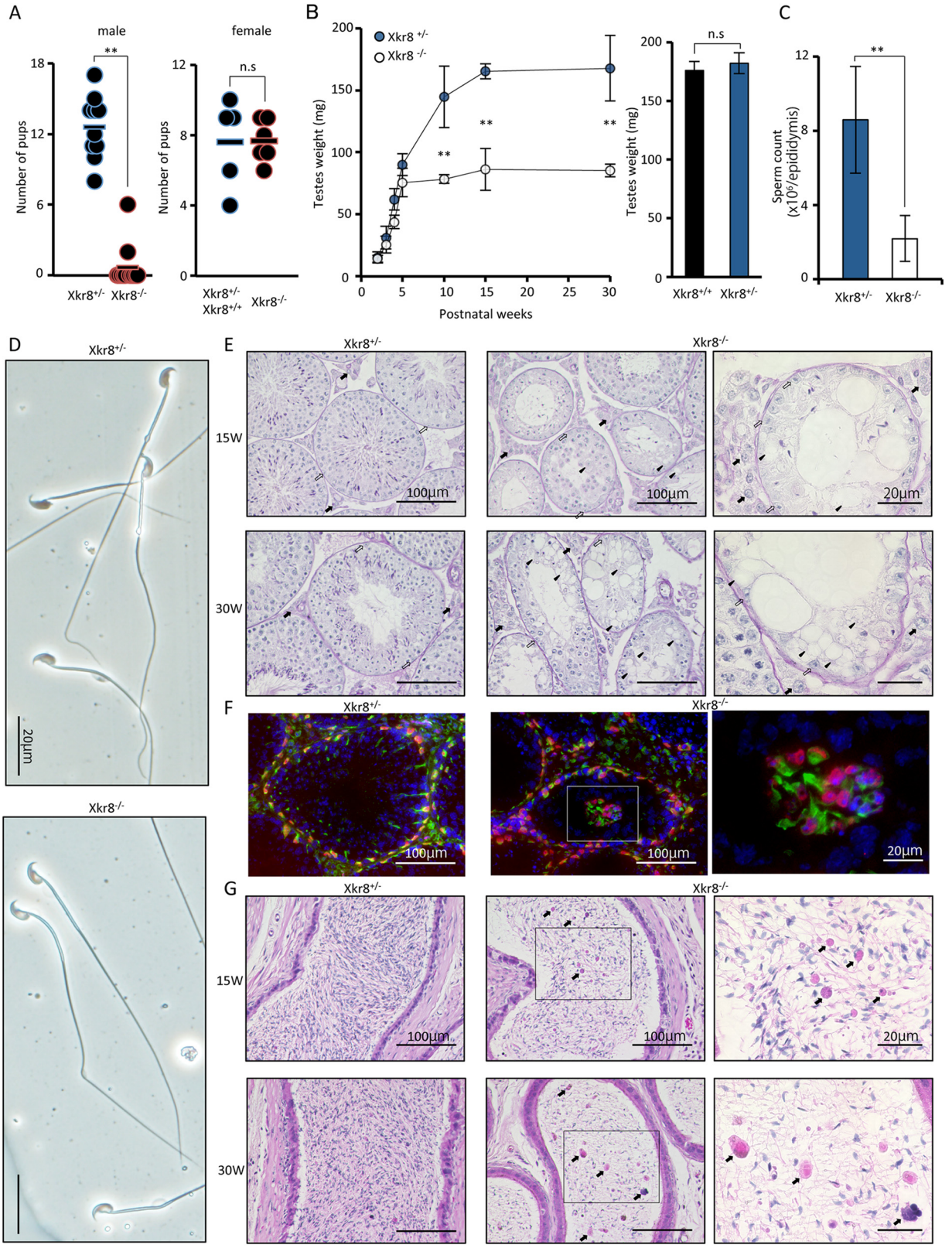

FIG 1 Impaired male fertility in *Xkr8*-null mice. (A) Male fertility. (Left) Male *Xkr8*$^{+/-}$ and *Xkr8*$^{-/-}$ mice ($n = 5$ for each) were mated with ICR female mice. Plugged female mice (10 to 12 for each genotype) were kept isolated, and the number of pups obtained from each was plotted. Bars show the average litter size. (Right) Female *Xkr8*$^{+/-}$ (or *Xkr8*$^{+/+}$) and *Xkr8*$^{-/-}$ mice ($n = 5$ for each) were mated with wild-type C57BL/6 male mice. The number of pups obtained from each female mouse was plotted. Bars show the average litter size. **, $P < 0.01$ (Student's *t* test). (B) Weight of the testes. (Left) The testes were removed from *Xkr8*$^{+/-}$ and *Xkr8*$^{-/-}$ mice ($n = 3$ to 6 each) at the indicated ages, and the average weight was plotted

(Continued on next page)

mice than in 15-week-old mice. Immunohistostaining analysis revealed aggregated vimentin-positive and Wilms' tumor 1 homolog (WT1)-positive Sertoli cells in the lumen of testicular tubules of Xkr8$^{-/-}$ (Fig. 1F). The epididymides of *Xkr8*$^{+/-}$ males at 15 weeks were full of mature sperm (Fig. 1G), while the sperm counts in *Xkr8*$^{-/-}$ epididymides were strongly reduced. *Xkr8*$^{-/-}$ epididymides showed more severe reductions in sperm number at 30 weeks and contained large amounts of amorphous eosinophilic materials, probably representing debris of dead cells or residual bodies released from maturing sperm. From these results, we concluded that *Xkr8* deficiency caused a defect in spermatogenesis and that fertility was impaired as a consequence of the reduced number of sperm.

Specific expression of Xkr8 in mouse testicular germ cells. Xkr8 is a member of the XK protein family (13). Among the 8 family members, Xkr4, Xkr8, and Xkr9 possess caspase-dependent scramblase activity (20). Real-time reverse transcription-PCR (RT-PCR) indicated that the testes of 5-week-old mice expressed Xkr8 mRNA but not XKR4 or XKR9 at an extremely high level. That is, its expression level in the testis was 100 to 1,000 times greater than that in the thymus or ovary (Fig. 2A). The testes are composed of germ cells, Sertoli cells, and Leydig cells, and the number of germ cells increases after birth (24, 25). In *W*/*W*^{v} mice, germ cells in the testes cannot proliferate due to mutation of the KIT proto-oncogene receptor tyrosine kinase (26). The expression levels of WT1 and of hydroxy-delta-5-steroid dehydrogenase, 3 beta- and steroid delta-isomerase 1 (HSD3B1), which are specifically expressed in Sertoli cells (27) and Leydig cells (28), respectively, were higher in *W*/*W*^{v} testes than in wild-type testes at 5 weeks (Fig. 2B). Conversely, the Xkr8 mRNA level in the testes of *W*/*W*^{v} mice was $<$10% of that in wild-type mice. This expression pattern is similar to that observed for DEAD box polypeptide 4 (DDX4; also called mouse VASA homolog) (Fig. 2B), which is expressed in germ cells (29), indicating that *Xkr8* is more strongly expressed in testicular germ cells than in somatic cells. The sharp increase in Xkr8 mRNA levels observed in the testes from 2 weeks after birth (Fig. 2C) was consistent with this idea. To further characterize *Xkr8* gene expression in testicular germ cells, testes were analyzed by *in situ* hybridization. As shown in Fig. 2D, experiments employing the antisense probe for Xkr8 mRNA, but not the sense probe, resulted in strong signals in germ cells, while no specific signals were detected in Sertoli or Leydig cells, confirming that *Xkr8* is specifically expressed in the germ cells, probably from the beginning of spermatogenesis.

Inefficient clearance of apoptotic cells in *Xkr8*$^{-/-}$ testes. During spermatogenesis, a large number of sperm progenitor cells undergo apoptosis and are engulfed by Sertoli cells in a PtdSer-dependent manner (17, 30, 31). Since Xkr8 is responsible for apoptotic PtdSer exposure in various cells (32), we hypothesized that *Xkr8*$^{-/-}$ apoptotic germ cells may not be efficiently cleared in the testes. As shown in Fig. 3A, approximately 2% of 4′,6-diamidino-2-phenylindole (DAPI)-positive cells in the testes of *Xkr8*$^{+/-}$ mice were positive by terminal deoxynucleotidyltransferase-mediated dUTP-biotin nick end labeling (TUNEL) at 2 to 4 weeks (Fig. 3A); this proportion increased by 67% in *Xkr8*$^{-/-}$ mice. Electron transmission microscopy demonstrated that most of the dead cells in *Xkr8*$^{+/-}$ testes were inside Sertoli cells and that their nuclei were swollen and degenerated (Fig. 3B). Conversely, dead cells in *Xkr8*$^{-/-}$ testes were outside Sertoli cells and contained condensed nuclei, indicating the presence of unengulfed apoptotic cells.

FIG 1 Legend (Continued)
with the standard deviation (SD) for each genotype. (Right) The average weight of the testes of 16-week-old *Xkr8*$^{+/+}$ and *Xkr8*$^{+/-}$ mice ($n = 3$ for each) was plotted with the SD (bars). **, $P < 0.01$ (Student's *t* test). (C and D) Analysis of sperm. Sperm were recovered from the cauda epididymides of *Xkr8*$^{+/-}$ and *Xkr8*$^{-/-}$ mice ($n = 9$ to 10 each) at 14 to 17 weeks, and the average numbers were plotted with the SD (bars) (C) and observed by microscopy (D). **, $P < 0.01$ (Student's *t* test). (E and G) Histochemical analysis. Paraffin sections were prepared from the testes (E) or cauda epididymides (G) of 15- or 30-week-old *Xkr8*$^{+/-}$ and *Xkr8*$^{-/-}$ mice, stained with PAS (E) or H&E (G), and observed by microscopy. In panel E, Sertoli and Leydig cells are indicated by open and closed arrows, respectively. Aggregated cells and vacuoles are indicated by arrowheads. In panel G, arrows indicate the debris of dead cells or residual bodies. (F) Cryosections were prepared from the testes of 8-week-old *Xkr8*$^{+/-}$ and *Xkr8*$^{-/-}$ mice and were stained with antivimentin (green), anti-Wt1 (red), and DAPI (blue).

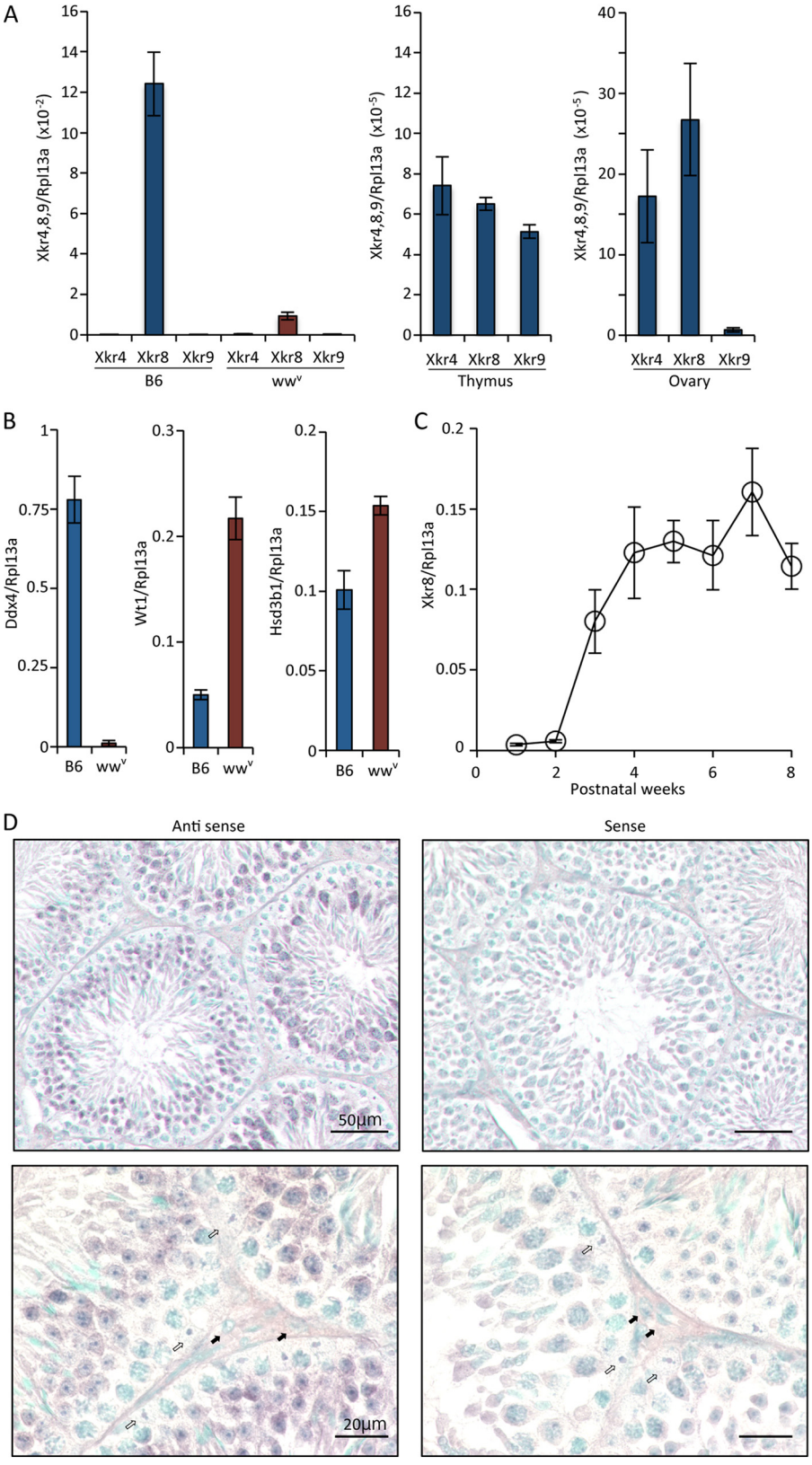

FIG 2 Expression of Xkr8 mRNA in testicular germ cells. (A and B) Real-time RT-PCR. Using RNA prepared from the testes, thymus, and ovary of 5-week-old wild-type or W/W^v mice ($n = 3$ for each), the mRNA levels of Xkr4, Xkr8, and Xkr9 (A) or of DDX4, WT1, and HSD3B1 (B) were measured by real-time RT-PCR. Ribosomal protein L13A (Rpl13a) was used for normalization of relative expression levels. Values shown represent averages of results from three mice and are presented with the SD (bars). (C) Age-dependent expression of

(Continued on next page)

When apoptotic cells are engulfed by phagocytes, their DNA is digested by DNase II in phagocyte lysosomes (33). We previously observed that a large amount of undigested naked DNA accumulated in the macrophages of *DNase II*-deficient mice (33). To confirm that apoptotic germ cells were not engulfed by Sertoli cells in the testes of *Xkr8*$^{-/-}$ mice, *Xkr8* and *DNaseII* doubly deficient mice were established in an interferon (alpha and beta) receptor 1 (*Ifnar1*)-deficient background (34). As shown in Fig. 3C, many abnormal foci of various sizes were observed in *Xkr8*$^{+/-}$ *DNaseII*$^{-/-}$ testes at the peripheral regions of the testicular tubes, where the Sertoli cells localized. Materials in the foci were weakly stained by hematoxylin but not by eosin, suggesting that inclusions in the foci mainly represented protein-free DNA generated in DNase II-deficient lysosomes. In *Xkr8*$^{-/-}$ *DNaseII*$^{-/-}$ testes, abnormal foci were less abundant (Fig. 3C), but many clusters of hematoxylin-positive materials were present in the peripheral regions of the testicular tubes, suggesting that these represented unengulfed apoptotic bodies with condensed and fragmented nuclei.

Xkr8 is required for PtdSer exposure in apoptotic testicular germ cells. The results described above suggested that Xkr8 is indispensable for the clearance of apoptotic germ cells in the testes. To confirm this, germ cell-rich fractions were prepared and treated with the apoptosis inducer ABT-737, a BH3 mimetic (35). Cells were then stained with fluorescently labeled annexin V and analyzed by flow cytometry to detect PtdSer exposure. *Xkr8*$^{+/-}$ germ cells exposed PtdSer in a dose- and time-dependent manner, and treatment with 10 μM ABT-737 for 60 min caused PtdSer exposure in >80% of germ cells (Fig. 4A and B). Conversely, 10 μM ABT-737 did not induce PtdSer exposure in *Xkr8*$^{-/-}$ germ cells, even after 90 min.

To confirm PtdSer exposure in apoptotic germ cells, germ cells were purified by a Percoll density gradient procedure and treated with ABT-737. Confocal microscopy indicated that most of the annexin V-positive cells were propidium iodide (PI) negative and that PtdSer was uniformly distributed on the cell surface (Fig. 4C). However, PtdSer-positive cells were rarely detected among ABT-737-treated *Xkr8*$^{-/-}$ germ cells and, when detected, were PI positive, indicating the presence of dead cells that had already undergone secondary necrosis (Fig. 4C). Western blotting indicated that caspase 3 was activated in *Xkr8*$^{-/-}$ germ cells upon ABT-737 treatment as efficiently as in *Xkr8*$^{+/-}$ cells (Fig. 4D). In addition, cleavage of poly(ADP-ribose) polymerase 1 (PARP1), a substrate of caspase 3 (36), was observed in ABT-737-treated *Xkr8*$^{-/-}$ germ cells at a level similar to that seen with the *Xkr8*$^{+/-}$ cells. These results indicated that *Xkr8*$^{+/-}$ and *Xkr8*$^{-/-}$ germ cells had the same sensitivity to the apoptosis inducer and that Xkr8 functions downstream of caspase 3.

We previously established NIH 3T3 cell transformants expressing MER proto-oncogene tyrosine kinase (MER) and T cell immunoglobulin and mucin domain-containing 4 (TIM4) (TKO-TIM4/MER) and demonstrated that the transformants efficiently engulfed PtdSer-presenting apoptotic cells (37). We therefore used this system to examine whether *Xkr8*$^{-/-}$ apoptotic germ cells can be engulfed by phagocytes. Germ cell-rich fractions were labeled with CellTracker Orange {9′-(4[and 5]-chloromethyl-2-carboxyphenyl)-7′-chloro-6′-oxo-1,2,2,4-tetramethyl-1,2-dihydropyrido[2′,3′-6]xanthene (CMRA)}, treated with ABT-737, and incubated at 37°C for 60 min with TKO-TIM4/MER cells at a prey/phagocyte ratio of 3:1. When the Xkr8$^{+/-}$ apoptotic germ cells were used as prey, confocal microscopy revealed that approximately 8.6% of the phagocytes contained CMRA-labeled materials (Fig. 4E). This proportion of CMRA-positive phagocytes was reduced to 4.1% with *Xkr8*$^{-/-}$ apoptotic germ cells, confirming that Xkr8-mediated PtdSer exposure plays an important role in the clearance of apoptotic testicular germ cells.

FIG 2 Legend (Continued)
Xkr8 mRNA in the testes. Testes were prepared from wild-type mice at the indicated ages ($n = 3$ for each age), and the Xkr8 mRNA level was measured by real-time RT-PCR. The average expression level of Xkr8, relative to RPL13A, was plotted with the SD (bars). (D) *In situ* hybridization for Xkr8 mRNA. Paraffin sections from the testes of 8-week-old wild-type mice were hybridized to DIG-labeled antisense or sense RNA, counterstained with methyl green, and observed by microscopy. Sertoli cells and Leydig cells are indicated by open and closed arrows, respectively.

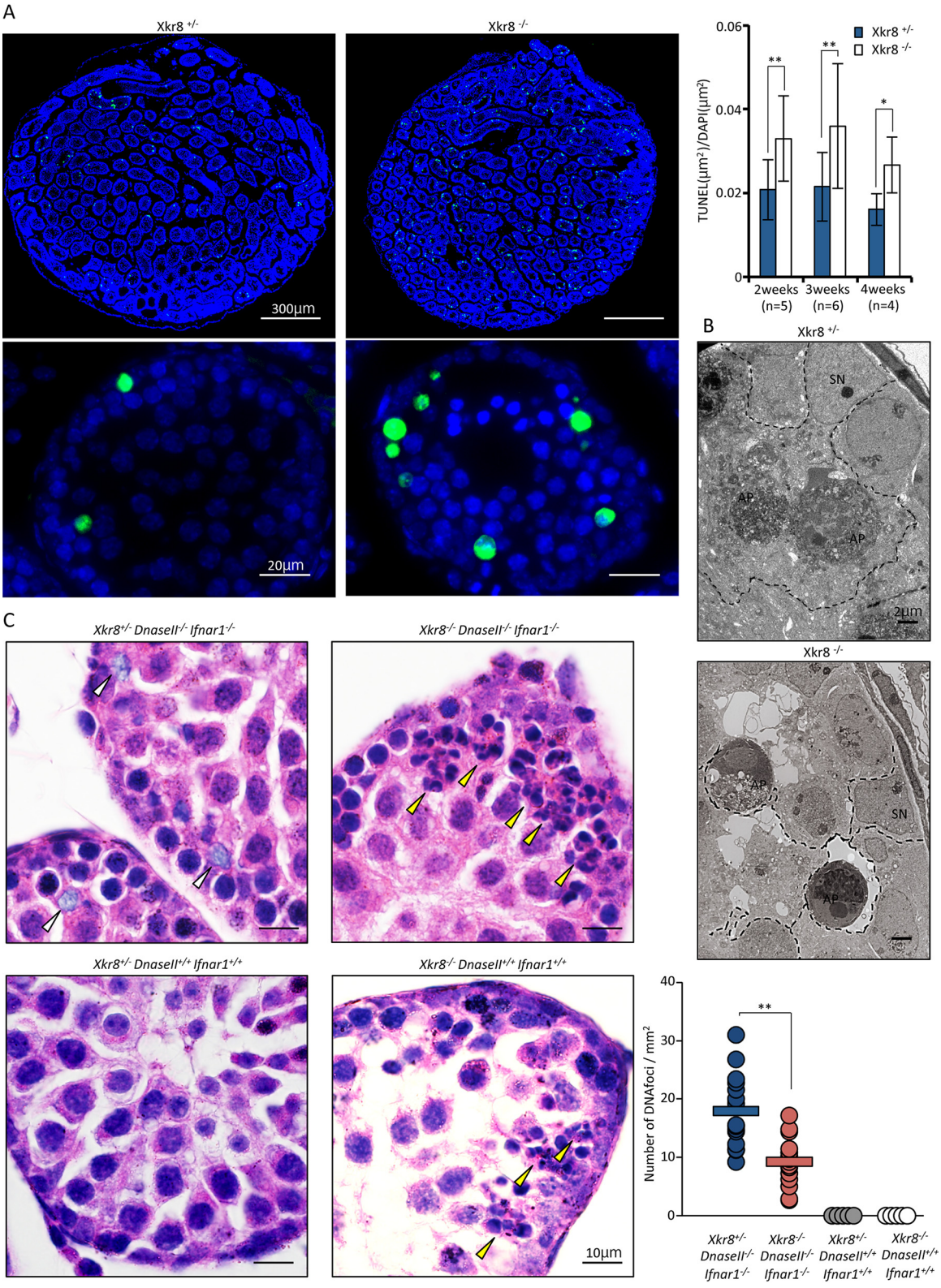

FIG 3 Inefficient clearance of apoptotic cells in *Xkr8*-null testes. (A) TUNEL staining of the testes. Results of TUNEL staining of testicular sections from 3-week-old *Xkr8*$^{+/-}$ and *Xkr8*$^{-/-}$ mice are shown at two magnifications. Green, TUNEL; blue, DAPI. (Left) Sections of the testes of mice of the indicated ages ($n = 4$ to 6 for each genotype) were processed for TUNEL assays and stained with DAPI. The total TUNEL-positive area was quantified from 3 to 5 sections per mouse, and the ratio of the DAPI-positive area and SD (bars) are shown. **, $P < 0.01$; *, $P < 0.05$ (Student's *t* test). (B) Electron microscopy of the testes. Sections of the testes of 3-week-old *Xkr8*$^{+/-}$ and *Xkr8*$^{-/-}$ mice were analyzed by transmission electron microscopy. Sertoli cells are indicated by dashed lines. SN, nuclei of Sertoli cells; AP, apoptotic cells. (C) *In vivo* efferocytosis revealed with DNase II-null mice. (Left) Paraffin sections of the testes of 3-week-old *Xkr8*$^{+/-}$ *DNaseII*$^{-/-}$

(Continued on next page)

DISCUSSION

Between embryonic day 10.5 (E10.5) and E11.5, primordial germ cells move into the gonadal ridge and proliferate. Spermatogenesis begins in the testes in the second week after birth and consists of spermatogonia proliferation, meiosis, spermatid formation, elongation, and shedding of cytoplasmic portions as residual bodies (38). This process absolutely depends on cell-cell contacts and paracrine interactions with Sertoli cells (39, 40). During spermatogenesis, up to 75% of germ cells undergo apoptosis, probably to maintain the ratio between germ cells and Sertoli cells (41, 42). Apoptotic germ cells display PtdSer and are engulfed by Sertoli cells and degraded in a PtdSer-dependent manner (19).

Xkr8 is a phospholipid scramblase that is activated by caspase cleavage and is responsible for apoptotic PtdSer exposure (10). Comparison of its mRNA levels in wild-type and W/W^v testes indicated that Xkr8 levels are at least 10 times higher in germ cells than in somatic cells. Similarly to many housekeeping genes (43), the promoter region of the mouse *Xkr8* gene is rich in CpG, and contains several *trans*-acting transcription factor 1 (SP1) binding sites. Two CpG islands are present near the transcriptional start site, and the expression of the human *Xkr8* gene is regulated by methylation and demethylation (13). The chromosomal DNA in both primordial germ cells and mature sperm is highly methylated. However, several germ line-specific genes are transiently demethylated and expressed after the germ cells migrate into the gonadal ridge (44). It is likely that *Xkr8* is also demethylated in male germ cells postmigration.

Apoptotic germ cells are engulfed by Sertoli cells in a PtdSer-dependent manner (19, 45). Scavenger receptor class B, member 1 (SCARB1) (46) and brain angiogenesis inhibitor (BAI1; also called adhesion G-protein coupled receptor B1) (45) have been proposed as receptors for exposed PtdSer on apoptotic germ cells. However, an analysis of single-cell RNA sequencing data from developing testes (47) indicated that BAI1 is not expressed in Sertoli cells, and both *Bai1*- and *Scarb1*-deficient male mice are fertile (48, 49). However, mRNAs of the TAM family tyrosine kinase receptors TYRO3 protein tyrosine kinase 3, MERTK, and AXL receptor tyrosine kinase are abundantly expressed in Sertoli cells (50). These receptors play redundant roles in engulfing apoptotic cells (37, 51, 52), and male mice lacking all three receptors are infertile (50), similarly to *Xkr8*-null mice. These results indicate that apoptotic germ cells exposing PtdSer through the actions of Xkr8 are engulfed by Sertoli cells via the TAM receptor system.

Both blocking and exaggeration of apoptosis in germ cells inhibit spermatogenesis and cause male infertility (53–57). As in the thymus, where more than 95% of thymocytes undergo apoptosis (58), apoptotic cells were barely detected in the testes of the wild-type mice, as they were efficiently engulfed and cleared by phagocytes in a PtdSer-dependent manner. We previously reported that Xkr8 deficiency causes a systemic lupus erythematosus-type autoimmune disease in a specific mouse strain (MRL) (32). This phenotype was accompanied by activation of the immune system and was observed only in aged female mice. Conversely, male infertility in *Xkr8*-deficient mice was not dependent on aging. Furthermore, neither inflammatory cells nor inflammatory cytokines were observed in the testes of *Xkr8*-null mice, indicating that the unengulfed dead cells themselves were responsible for infertility.

How can unengulfed apoptotic cells inhibit spermatogenesis? Unengulfed apoptotic cells undergo secondary necrosis and release cellular materials (7, 59), which may directly kill the germ cells. In addition, as some toxic substances are known to activate FasL on Sertoli cells (60), the Fas-FasL system may play a role to killing Fas-expressing

FIG 3 Legend (Continued)
Ifnar1$^{-/-}$, *Xkr8*$^{-/-}$ *DNaseII*$^{-/-}$ *Ifnar1*$^{-/-}$, *Xkr8*$^{+/-}$ *DNaseII*$^{+/+}$ *Ifnar1*$^{+/+}$, or *Xkr8*$^{-/-}$ *DNaseII*$^{+/+}$ *Ifnar1*$^{+/+}$ mice were stained with H&E and observed by microscopy. White arrowheads indicate Sertoli cells carrying undigested DNA (foci), while yellow arrowheads indicate unengulfed apoptotic cells. (Right) Foci were counted in 15 sections or 5 sections obtained from three mice per genotype and are expressed as a ratio to the total tissue area. The bars indicate average values. **, $P < 0.01$ (Student's *t* test).

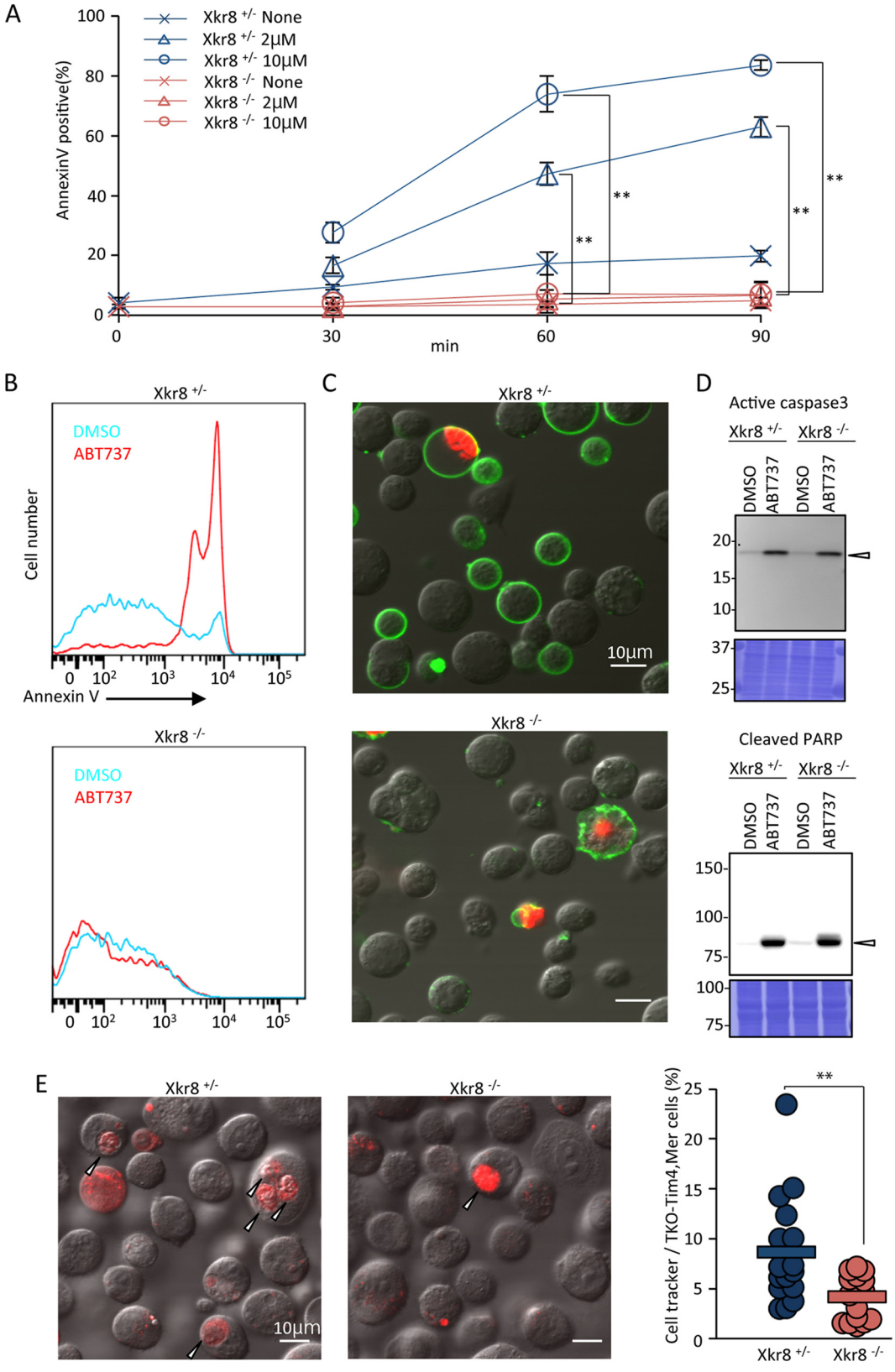

FIG 4 Inefficient apoptotic PtdSer exposure in *Xkr8*-null male germ cells. (A) Time course of the apoptotic PtdSer exposure in male germ cells. Germ cell-rich fractions prepared from the testes of *Xkr8*$^{+/-}$ and *Xkr8*$^{-/-}$ mice were treated for the indicated time periods with 0, 2, or 10 μM ABT-737, stained with Cy5-annexin V and PI, and analyzed by flow cytometry. Experiments were performed in triplicate, and the average percentages of annexin V-positive and PI-negative cells were plotted with the SD (bars). **, $P < 0.01$ (Student's *t* test). (B) Flow cytometry. Cells from *Xkr8*$^{+/-}$ and *Xkr8*$^{-/-}$ testes of 3-week-old mice were left

(Continued on next page)

germ cells. Alternatively, a more interesting possibility is that Sertoli cells, which use engulfed apoptotic germ cells as energy sources (61, 62), starve because of failure to engulf *Xkr8*-null apoptotic germ cells. These starved Sertoli cells may lose the ability to support second-round spermatogenesis. We observed many large vacuoles in the Sertoli cells of *Xkr8*-null testes, consistent with this notion. In addition to apoptotic germ cells, residual bodies are engulfed by Sertoli cells in a PtdSer-dependent manner (63). Residual body-like structures were observed in *Xkr8*-null epididymides, suggesting that Xkr8 is also involved in the PtdSer exposure of residual bodies. Whether Xkr8 is actually involved in the clearance of residual bodies remains to be confirmed.

MATERIALS AND METHODS

Mice. C57BL/6J mice were purchased from Japan CLEA or Japan SLC. W/W^{v} mice and ICR mice were purchased from Japan SLC. *Xkr8*$^{-/-}$ mice in the C57BL/6 background (13) and *DNaseII*$^{-/-}$ *Ifnar1*$^{-/-}$ mice (34) have been previously described and were crossed to generate *Xkr8*$^{-/-}$ *DNaseII*$^{-/-}$ *Ifnar1*$^{-/-}$ mice. All mice were housed in a specific-pathogen-free facility at the Research Institute for Microbial Diseases at Osaka University, and all mouse studies were approved by the Ethics Review Committee for Animal Experimentation of Research Institute for Microbial Diseases, Osaka University.

Cell lines and reagents. *Axl*$^{-/-}$ *Tyro3*$^{-/-}$ *Gas6*$^{-/-}$ NIH 3T3 cells expressing mouse TIM4 and MerTK (TKO-TIM4/MER) (37) were cultured in Dulbecco's modified Eagle's medium (DMEM) containing 10% fetal calf serum (FCS). CMRA was purchased from Life Technologies, ABT-737 from Sellec, Cy5-annexin V from Biovision, and iFluor 488-annexin V from AAT Bioquest.

Real-time RT-PCR. RNA was isolated using ISOGEN (Nippon Gene) and an RNeasy microkit (Qiagen) and was subjected to RT with a High Capacity RNA-to-cDNA kit (Thermo Fisher Scientific). An aliquot of the product was amplified by PCR in a reaction mixture containing LightCycler 480 SYBR green master (Roche). The mouse primers used for real-time RT-PCR were as follows: for *Xkr8*, 5′-GCGACGCCACAGCTCACACT-3′ and 5′-CCCCAGCAGCAGCAGGTTCC-3′; for *Xkr4*, 5′-GCCAGTGACCGTGATCAGAA-3′ and 5′-TCCTTGTACTGCAGCCTTGG-3′; for *Xkr9*, 5′-GGAAGGCTGCCCGCAACTCA-3′ and 5′-TGGGCCAGAGTCCTCGGAGAA-3′; for *Ddx4*, 5′-CTGTCAGACGCTCAACAGGA-3′ and 5′-CGCTGTATTCAACGTGTGCT-3′; for *Wt1*, 5′-TCCGGTCAGCATCTGAAACC-3′ and 5′-GAGCTGGTCTGAGCGAGAAA-3′; for *Hsd3b1*, 5′-TCCAAGCTGCAGACAAAGACC-3′ and 5′-ACACAGGCCTCCAATAGGTTC-3′; and for *Rpl13a*, 5′-CCCTCCACCCTATGACAAGA-3′ and 5′-TTCTCCTCCAGAGTGGCTGT-3′.

Isolation of male germ cells. Male germ cells were isolated as described previously (64, 65) with some modifications. In brief, testes were dissected from 3-week-old mice and their tunica albugineae were removed. These were placed in 15-ml conical centrifuge tubes containing 5 ml of Hanks' balanced salt solution (HBSS) containing 120 U/ml collagenase type 4 (Worthington) and 5 μg/ml DNase I. After vigorous shaking at room temperature to loosen the seminiferous tubules, samples were incubated for 15 min at 37°C, washed twice with 5 ml HBSS, and digested at 37°C for 15 min with 0.025% trypsin–5 μg/ml DNase I–HBSS. After quenching was performed with 500 μl FCS, the cell suspension was passed through a 40-μm-pore-size nylon mesh strainer. The cells were then collected by centrifugation at 400 $\times$ *g* for 5 min and suspended in DMEM containing 10% FCS. For microscopic observation and assays for engulfment of apoptotic cells (efferocytosis), germ cells were further purified by the use of a discontinuous Percoll density gradient procedure (65, 66). Isotonic Percoll solutions with different osmolarities were prepared from a stock solution consisting of 9 parts Percoll II Plus (GE Healthcare) and 1 part 10$\times$ HBSS containing 2% FCS and 2 μg/ml DNase I. The Percoll stock solution (100%) was diluted with HBSS containing 2% FCS and 2 μg/ml DNase I to 15, 22, 30, 36, and 40%. Gradients were prepared in 15-ml conical centrifuge tubes by gently layering 1 ml of each, starting with the 40% fraction. Male germ cell suspensions (1 ml) were applied to the top layers of the gradient tubes, and the tubes were centrifuged at 800 $\times$ *g* for 20 min at 16°C. Cells between the 30 and 40% layers were collected, washed with HBSS, and suspended in DMEM containing 10% FCS.

Induction of apoptosis, PtdSer exposure, and caspase activation. Male germ cells were induced to undergo apoptosis with ABT-737 as described previously (32). In brief, cells (8×10^5/ml) were incubated at 37°C for 60 min with 10 μM ABT-737–HBSS. The cells were washed with annexin V buffer (10 mM HEPES-NaOH buffer [pH 7.4], 140 mM NaCl, and 1 mM $CaCl_2$), stained on ice for 5 min with 1,000-fold-diluted Cy5-annexin V and 5 μg/ml PI, and analyzed on a FACSCanto flow cytometer (BD). In

FIG 4 Legend (Continued)
untreated or treated with 10 μM ABT-737, stained with Cy5-annexin V and PI, and analyzed by flow cytometry. Annexin V-staining profiles in the PI-negative germ cell fraction are shown. (C) Fluorescence microscopy. Germ cells from *Xkr8*$^{+/-}$ and *Xkr8*$^{-/-}$ mice were purified by density gradient centrifugation, treated with 5 μM ABT-737, stained with iFluor 488-annexin V and PI, and observed by confocal fluorescence microscopy. (D) Activation of caspase 3. Testicular germ cells were incubated with or without 10 μM ABT-737, and the cell lysates (16 μg protein) were analyzed by Western blotting. The arrowheads indicate active caspase 3 (top) and cleaved PARP (bottom). (Lower panel) Membranes were stained with Coomassie brilliant blue. (E) *In vitro* efferocytosis. Testicular germ cells were labeled with CMRA, treated with 5 μM ABT-737, and then incubated with TKO-TIM4/MER cells. After incubation, TKO cells were observed by confocal fluorescence microscopy. (Right) CMRA-positive engulfed cells were counted in 16 different fields obtained in three independent experiments, and data are expressed as ratios to the number of phagocytes. The bars indicate the average values. **, $P < 0.01$ (Student's *t* test).

some cases, samples were stained with 200-fold-diluted iFluor 488-annexin–5 μg/ml PI–annexin V buffer and were observed on a FluoView FV1000 confocal microscope (Olympus).

To detect activated caspase 3, cells treated with ABT-737 were washed with phosphate-buffered saline (PBS) and lysed in radioimmunoprecipitation assay (RIPA) buffer (50 mM HEPES-NaOH buffer [pH 8.0] containing 1% Nonidet P-40, 1% SDS, 0.5% sodium deoxycholate, and 150 mM NaCl) supplemented with a mixture of protease inhibitors (cOmplete Mini; Sigma-Aldrich). The lysates were centrifuged at 20,000 $\times$ *g* for 20 min to remove debris, mixed with a 1/4 volume of 5$\times$ SDS sample buffer (200 mM Tris-HCl buffer [pH 6.8], 10% [wt/vol] SDS, 25% [vol/vol] glycerol, 5% [vol/vol] β-mercaptoethanol, and 0.05% bromophenol blue), incubated at room temperature for 30 min, and subjected to 10-to-20% gradient SDS-PAGE (Bio Craft). Proteins were transferred to polyvinylidene difluoride membranes (Merck), blocked at room temperature for 1 h with blocking buffer (25 mM Tris-HCl buffer [pH 7.5] containing 5% skim milk and 0.05% Tween 20), and incubated at 4°C overnight with rabbit anti-cleaved caspase 3 or anti-cleaved PARP antibodies (Cell Signaling Technology). Membranes were then incubated with horseradish peroxidase (HRP)-labeled goat anti-rabbit IgG (Dako), and peroxidase activity was detected with Immobilon Western chemiluminescent HRP substrate (Merck).

Efferocytosis. Efferocytosis assays were performed essentially as previously described (37). In brief, germ cells were incubated with 2 μM CMRA–PBS at 37°C for 20 min and were treated with 5 μM ABT-737–DMEM–10% FCS at 37°C for 60 min. The cells were collected by centrifugation at 400 $\times$ *g* for 5 min and suspended in DMEM–10% FCS. CMRA-labeled prey cells (3×10^5 cells) were then incubated with 1×10^5 TKO-TIM4/MER cells (37) in a mixture containing 500 μl of DMEM–10% FCS at 37°C for 60 min. After a washing with PBS, the phagocytes were detached with 0.25% trypsin–PBS–1 mM EDTA by incubation at 37°C for 3 min, collected by centrifugation, suspended in 300 μl of PBS containing 2% FCS, and analyzed by confocal microscopy on glass-bottom dishes (IWAKI).

***In situ* hybridization.** To prepare a digoxigenin (DIG)-labeled probe for *in situ* hybridization, a 500-bp DNA fragment (nucleotides 1021 to 1520) of mouse Xkr8 cDNA (NP_95876) was prepared by PCR using the primers 5′-GGGATCTCATTGCTGATGTG-3′ and 5′-GGGTAGGGAAGAGTTCTCCC-3′ and was inserted into pGEMT-Easy vector (Promega) in two orientations. DIG-labeled probes were synthesized by *in vitro* transcription using T7 polymerase (Roche). *In situ* hybridization was performed according to the method of Nomura et al. (67) using a kit from Genostaff. In brief, the testes of 8-week-old mice was incubated in 0.1 M sodium phosphate buffer (pH 7.0) containing 10% neutral buffered formalin (NBF) at room temperature for 2 days and gradually dehydrated by immersion in 70, 80, and 90% ethanol for 1.5 h each time and then twice in 100% ethanol for 1.5 h. After soaking in a 1:1 mixture of ethanol and xylene for 1.5 h and three times in 100% xylene for 1.5 h, samples were incubated in paraffin three times for 1.5 h each time at 60°C, sliced into 6-μm-thick sections using a microtome (RM2245; Leica), and mounted on MAS-coated slides (Matsunami). The sections were deparaffinized with xylene and rehydrated with a graded series of ethanol (twice with 100%, once each with 90, 80, and 70% ethanol, and then once with water), rinsed with PBS, refixed with 10% NBF at 37°C for 30 min, and washed three times with water. The sections were then incubated in 0.08 N HCl at 37°C for 10 min, washed once with water and twice with PBS, and treated with 3 μg/ml proteinase K–PBS at 37°C for 10 min. After two washes with PBS, the sections were rinsed with 1$\times$ G-WASH (Genostaff) and hybridized with 1 μg/ml RNA probe–G-HyboL (Genostaff) at 60°C for 16 h. The sections were successively incubated at 60°C for 10 min each time in 1$\times$ G-WASH and in 1$\times$ G-WASH containing 50% formamide, twice in 1$\times$ G-WASH, and twice in 0.1$\times$ G-WASH. After two washes performed with Tris-buffered saline (TBS) containing 0.1% Tween 20 (TBST) at room temperature for 5 min, sections were incubated at room temperature for 15 min in G-Block (Genostaff) and then with 2,000-fold-diluted alkaline phosphatase-conjugated anti-DIG antibody (Roche) diluted in TBST containing 2% G-block for 60 min. The sections were washed twice with TBST for 10 min at room temperature, and the signals were visualized by incubation with 200 ng/ml nitrotetrazolium blue chloride (Sigma) and 50 ng/ml 5-bromo-4-chloro-3-indolylphosphate disodium salt (Sigma) in a mixture containing 0.1 M Tris-HCl buffer (pH 9.5), 0.1 M NaCl, and 50 mM $MgCl_2$ at 4°C overnight. After a washing with PBS, the sections were counterstained with 0.02% methyl green and mounted with G-Mount (Genostaff).

Histological analysis. Testes and epididymides were fixed at room temperature for 24 h in Bouin solution (Wako) and in PBS containing 4% paraformaldehyde (PFA), respectively. Samples were then soaked overnight in 70% ethanol, dehydrated, embedded in paraffin, sectioned at 4 μm, and mounted on glass slides as described above. The sections were then deparaffinized, rehydrated, stained with periodic acid-Schiff (PAS) stain or with hematoxylin and eosin (H&E), and observed on a BioRevo BZ-9000 fluorescence microscope (Keyence).

Immunohistological staining. Testes were mounted in OCT embedding compound (Sakura Finetek) and frozen at −80°C. Tissues were sliced at 6 μm and fixed with 4% PFA. The sections were then permeabilized at room temperature for 30 min with PBS containing 0.1% Triton-X and 2% FCS and incubated at room temperature for 60 min with chicken anti-vimentin (Merck Millipore) and rabbit anti-Wt1 (Abcam). Sections were then incubated with Alexa Fluor 488-conjugated goat anti-chicken IgY and Alexa Fluor 555-conjugated goat anti-rabbit IgG (Invitrogen) and were observed on a BioRevo BZ-9000 fluorescence microscope (Keyence).

TUNEL staining and quantification of phagocytes carrying undigested DNA. For TUNEL staining, testes were fixed with 4% PFA, embedded in paraffin, and sliced in 6-μm sections as described above. TUNEL staining was performed using an ApopTag *in situ* apoptosis detection kit (Merck Millipore). After staining, sections were counterstained with DAPI, mounted with FluorSave (Merck Millipore), and observed by fluorescence microscopy (BioRevo BZ9000). TUNEL- and DAPI-positive

areas were measured using a BZ-II analyzer (Keyence). To detect phagocytes carrying undigested DNA, the testes of 3-week-old mice were fixed with 4% PFA–PBS at room temperature for 24 h, embedded in paraffin, and sliced into 6-μm sections. Sections were stained with H&E and observed by microscopy. Phagocytes carrying DNA were quantified for each genotype.

Sperm counts. Sperm from the cauda epididymides were collected in 1 ml PBS, diluted 10-fold with water to stop their movement, and counted with a hemocytometer.

Electron transmission microscopy. Mice were anesthetized, and the testes were fixed by cardiac perfusion with 50 ml of 2% glutaraldehyde–2% PFA–0.1 M sodium phosphate buffer (pH 7.4). The testes were excised and subjected to additional fixation in the same solution at 4°C for 24 h, postfixed with 1% OsO_4 at 4°C for 2 h, and dehydrated by immersion in a graded ethanol series. After two 20-min immersions in 100% ethanol, the samples were incubated at room temperature twice in propylene oxide for 20 min, in a 3:1 mixture of propylene oxide and epoxide for 1 h, in a 1:3 mixture of propylene oxide and epoxide for 1 h, and in epoxide overnight. They were then embedded in epoxide by incubation at 60°C for 3 days. Ultrathin sections (70 to 80 nm) were prepared with an Ultracut UCT ultramicrotome (Leica), stained with uranyl acetate and lead citrate, and observed on a H-7650 microscope (Hitachi High-Technologies).

ACKNOWLEDGMENTS

We thank J. Suzuki for the help at the initial stage of the study and M. Fujii for administrative assistance. We thank M. Ikawa and H. Miyata for their opinions.

This work was supported by grants from the Japan Science Promotion Society (15H05785 to S.N.) and from Japan Science Technology (JPMJCR14M4 to S.N.).

We declare that we have no conflicts of interest.

REFERENCES

1. Fuchs Y, Steller H. 2015. Live to die another way: modes of programmed cell death and the signals emanating from dying cells. Nat Rev Mol Cell Biol 16:329–344. https://doi.org/10.1038/nrm3999.
2. Jorgensen I, Rayamajhi M, Miao EA. 2017. Programmed cell death as a defence against infection. Nat Rev Immunol 17:151–164. https://doi.org/10.1038/nri.2016.147.
3. Prager I, Watzl C. 2019. Mechanisms of natural killer cell-mediated cellular cytotoxicity. J Leukoc Biol 105:1319–1329. https://doi.org/10.1002/JLB.MR0718-269R.
4. Galluzzi L, Vitale I, Aaronson SA, Abrams JM, Adam D, Agostinis P, Alnemri ES, Altucci L, Amelio I, Andrews DW, Annicchiarico-Petruzzelli M, Antonov AV, Arama E, Baehrecke EH, Barlev NA, Bazan NG, Bernassola F, Bertrand MJM, Bianchi K, Blagosklonny MV, Blomgren K, Borner C, Boya P, Brenner C, Campanella M, Candi E, Carmona-Gutierrez D, Cecconi F, Chan FK-M, Chandel NS, Cheng EH, Chipuk JE, Cidlowski JA, Ciechanover A, Cohen GM, Conrad M, Cubillos-Ruiz JR, Czabotar PE, D'Angiolella V, Dawson TM, Dawson VL, De Laurenzi V, De Maria R, Debatin K-M, DeBerardinis RJ, Deshmukh M, Di Daniele N, Di Virgilio F, et al. 2018. Molecular mechanisms of cell death: recommendations of the Nomenclature Committee on Cell Death 2018. Cell Death Differ 25:486–541. https://doi.org/10.1038/s41418-017-0012-4.
5. Riedl SJ, Salvesen GS. 2007. The apoptosome: signalling platform of cell death. Nat Rev Mol Cell Biol 8:405–413. https://doi.org/10.1038/nrm2153.
6. Crawford ED, Seaman JE, Agard N, Hsu GW, Julien O, Mahrus S, Nguyen H, Shimbo K, Yoshihara HAI, Zhuang M, Chalkley RJ, Wells JA. 2013. The DegraBase: a database of proteolysis in healthy and apoptotic human cells. Mol Cell Proteomics 12:813–824. https://doi.org/10.1074/mcp.O112.024372.
7. Nagata S. 2018. Apoptosis and the clearance of apoptotic cells. Annu Rev Immunol 36:489–517. https://doi.org/10.1146/annurev-immunol-042617-053010.
8. Savill J, Fadok V. 2000. Corpse clearance defines the meaning of cell death. Nature 407:784–788. https://doi.org/10.1038/35037722.
9. Muñoz LE, Lauber K, Schiller M, Manfredi AA, Herrmann M. 2010. The role of defective clearance of apoptotic cells in systemic autoimmunity. Nat Rev Rheumatol 6:280–289. https://doi.org/10.1038/nrrheum.2010.46.
10. Nagata S, Suzuki J, Segawa K, Fujii T. 2016. Exposure of phosphatidylserine on the cell surface. Cell Death Differ 23:952–961. https://doi.org/10.1038/cdd.2016.7.
11. Bevers EM, Williamson PL. 2016. Getting to the outer leaflet: physiology of phosphatidylserine exposure at the plasma membrane. Physiol Rev 96:605–645. https://doi.org/10.1152/physrev.00020.2015.
12. Birge RB, Boeltz S, Kumar S, Carlson J, Wanderley J, Calianese D, Barcinski M, Brekken RA, Huang X, Hutchins JT, Freimark B, Empig C, Mercer J, Schroit AJ, Schett G, Herrmann M. 2016. Phosphatidylserine is a global immunosuppressive signal in efferocytosis, infectious disease, and cancer. Cell Death Differ 23:962–978. https://doi.org/10.1038/cdd.2016.11.
13. Suzuki J, Denning DP, Imanishi E, Horvitz HR, Nagata S. 2013. Xk-related protein 8 and CED-8 promote phosphatidylserine exposure in apoptotic cells. Science 341:403–406. https://doi.org/10.1126/science.1236758.
14. Segawa K, Kurata S, Yanagihashi Y, Brummelkamp T, Matsuda F, Nagata S. 2014. Caspase-mediated cleavage of phospholipid flippase for apoptotic phosphatidylserine exposure. Science 344:1164–1168. https://doi.org/10.1126/science.1252809.
15. Segawa K, Kurata S, Nagata S. 2016. Human type IV P-type ATPases that work as plasma membrane phospholipid flippases, and their regulation by caspase and calcium. J Biol Chem 291:762–772. https://doi.org/10.1074/jbc.M115.690727.
16. Shaha C, Tripathi R, Mishra DP. 2010. Male germ cell apoptosis: regulation and biology. Philos Trans R Soc Lond B Biol Sci 365:1501–1515. https://doi.org/10.1098/rstb.2009.0124.
17. Nakanishi Y, Shiratsuchi A. 2004. Phagocytic removal of apoptotic spermatogenic cells by Sertoli cells: mechanisms and consequences. Biol Pharm Bull 27:13–16. https://doi.org/10.1248/bpb.27.13.
18. Chemes H. 1986. The phagocytic function of Sertoli cells: a morphological, biochemical, and endocrinological study of lysosomes and acid phosphatase localization in the rat testis. Endocrinology 119:1673–1681. https://doi.org/10.1210/endo-119-4-1673.
19. Shiratsuchi A, Umeda M, Ohba Y, Nakanishi Y. 1997. Recognition of phosphatidylserine on the surface of apoptotic spermatogenic cells and subsequent phagocytosis by Sertoli cells of the rat. J Biol Chem 272:2354–2358. https://doi.org/10.1074/jbc.272.4.2354.
20. Suzuki J, Imanishi E, Nagata S. 2014. Exposure of phosphatidylserine by Xk-related protein family members during apoptosis. J Biol Chem 289:30257–30267. https://doi.org/10.1074/jbc.M114.583419.
21. Bechard A, Nicholson A, Mason G. 2012. Litter size predicts adult stereotypic behavior in female laboratory mice. J Am Assoc Lab Anim Sci 51:407–411.
22. Platt KM, Charnigo RJ, Kincer JF, Dickens BJ, Pearson KJ. 2013. Controlled exercise is a safe pregnancy intervention in mice. J Am Assoc Lab Anim Sci 52:524–530.
23. Mu X, Lee Y-F, Liu N-C, Chen Y-T, Kim E, Shyr C-R, Chang C. 2004. Targeted inactivation of testicular nuclear orphan receptor 4 delays and disrupts late meiotic prophase and subsequent meiotic divisions of spermatogenesis. Mol Cell Biol 24:5887–5899. https://doi.org/10.1128/MCB.24.13.5887-5899.2004.

24. Vergouwen RP, Huiskamp R, Bas RJ, Roepers-Gajadien HL, Davids JA, de Rooij DG. 1993. Postnatal development of testicular cell populations in mice. J Reprod Fertil 99:479–485. https://doi.org/10.1530/jrf.0.0990479.
25. Vergouwen RP, Jacobs SG, Huiskamp R, Davids JA, de Rooij DG. 1991. Proliferative activity of gonocytes, Sertoli cells and interstitial cells during testicular development in mice. J Reprod Fertil 93:233–243. https://doi.org/10.1530/jrf.0.0930233.
26. Mauduit C, Hamamah S, Benahmed M. 1999. Stem cell factor/c-kit system in spermatogenesis. Hum Reprod Update 5:535–545. https://doi.org/10.1093/humupd/5.5.535.
27. Pelletier J, Schalling M, Buckler AJ, Rogers A, Haber DA, Housman D. 1991. Expression of the Wilms's tumor gene WT1 in the murine urogenital system. Genes Dev 5:1345–1356. https://doi.org/10.1101/gad.5.8.1345.
28. Yokoyama C, Chigi Y, Baba T, Ohshitanai A, Harada Y, Takahashi F, Morohashi K-i. 2019. Three populations of adult Leydig cells in mouse testes revealed by a novel mouse HSD3B1-specific rat monoclonal antibody. Biochem Biophys Res Commun 511:916–920. https://doi.org/10.1016/j.bbrc.2019.02.100.
29. Tanaka SS, Toyooka Y, Akasu R, Katoh-Fukui Y, Nakahara Y, Suzuki R, Yokoyama M, Noce T. 2000. The mouse homolog of Drosophila Vasa is required for the development of male germ cells. Genes Dev 14:841–853.
30. Krishnamurthy H, Weinbauer GF, Aslam H, Yeung CH, Nieschlag E. 1998. Quantification of apoptotic testicular germ cells in normal and methoxyacetic acid-treated mice as determined by flow cytometry. J Androl 19:710–717.
31. Russell LD, Alger LE, Nequin LG. 1987. Hormonal control of pubertal spermatogenesis. Endocrinology 120:1615–1632. https://doi.org/10.1210/endo-120-4-1615.
32. Kawano M, Nagata S. 2018. Lupus-like autoimmune disease caused by a lack of Xkr8, a caspase-dependent phospholipid scramblase. Proc Natl Acad Sci U S A 115:2132–2137. https://doi.org/10.1073/pnas.1720732115.
33. Kawane K, Fukuyama H, Yoshida H, Nagase H, Ohsawa Y, Uchiyama Y, Okada K, Iida T, Nagata S. 2003. Impaired thymic development in mouse embryos deficient in apoptotic DNA degradation. Nat Immunol 4:138–144. https://doi.org/10.1038/ni881.
34. Yoshida H, Okabe Y, Kawane K, Fukuyama H, Nagata S. 2005. Lethal anemia caused by interferon-beta produced in mouse embryos carrying undigested DNA. Nat Immunol 6:49–56. https://doi.org/10.1038/ni1146.
35. van Delft MF, Wei AH, Mason KD, Vandenberg CJ, Chen L, Czabotar PE, Willis SN, Scott CL, Day CL, Cory S, Adams JM, Roberts AW, Huang D. 2006. The BH3 mimetic ABT-737 targets selective Bcl-2 proteins and efficiently induces apoptosis via Bak/Bax if Mcl-1 is neutralized. Cancer Cell 10:389–399. https://doi.org/10.1016/j.ccr.2006.08.027.
36. Crawford ED, Wells JA. 2011. Caspase substrates and cellular remodeling. Annu Rev Biochem 80:1055–1087. https://doi.org/10.1146/annurev-biochem-061809-121639.
37. Yanagihashi Y, Segawa K, Maeda R, Nabeshima Y-i, Nagata S. 2017. Mouse macrophages show different requirements for phosphatidylserine receptor Tim4 in efferocytosis. Proc Natl Acad Sci U S A 114:8800–8805. https://doi.org/10.1073/pnas.1705365114.
38. Griswold MD. 2016. Spermatogenesis: the commitment to meiosis. Physiol Rev 96:1–17. https://doi.org/10.1152/physrev.00013.2015.
39. França LR, Hess RA, Dufour JM, Hofmann MC, Griswold MD. 2016. The Sertoli cell: one hundred fifty years of beauty and plasticity. Andrology 4:189–212. https://doi.org/10.1111/andr.12165.
40. Kanatsu-Shinohara M, Shinohara T. 2013. Spermatogonial stem cell self-renewal and development. Annu Rev Cell Dev Biol 29:163–187. https://doi.org/10.1146/annurev-cellbio-101512-122353.
41. Baum JS, St George JP, McCall K. 2005. Programmed cell death in the germline. Semin Cell Dev Biol 16:245–259. https://doi.org/10.1016/j.semcdb.2004.12.008.
42. Print CG, Loveland KL. 2000. Germ cell suicide: new insights into apoptosis during spermatogenesis. Bioessays 22:423–430. https://doi.org/10.1002/(SICI)1521-1878(200005)22:5<423::AID-BIES4>3.0.CO;2-0.
43. Beishline K, Azizkhan-Clifford J. 2015. Sp1 and the 'hallmarks of cancer'. FEBS J 282:224–258. https://doi.org/10.1111/febs.13148.
44. Maatouk DM, Kellam LD, Mann MRW, Lei H, Li E, Bartolomei MS, Resnick JL. 2006. DNA methylation is a primary mechanism for silencing postmigratory primordial germ cell genes in both germ cell and somatic cell lineages. Development 133:3411–3418. https://doi.org/10.1242/dev.02500.
45. Elliott MR, Zheng S, Park D, Woodson RI, Reardon MA, Juncadella IJ, Kinchen JM, Zhang J, Lysiak JJ, Ravichandran KS. 2010. Unexpected requirement for ELMO1 in clearance of apoptotic germ cells in vivo. Nature 467:333–337. https://doi.org/10.1038/nature09356.
46. Kawasaki Y, Nakagawa A, Nagaosa K, Shiratsuchi A, Nakanishi Y. 2002. Phosphatidylserine binding of class B scavenger receptor type I, a phagocytosis receptor of testicular Sertoli cells. J Biol Chem 277:27559–27566. https://doi.org/10.1074/jbc.M202879200.
47. Ernst C, Eling N, Martinez-Jimenez CP, Marioni JC, Odom DT. 2019. Staged developmental mapping and X chromosome transcriptional dynamics during mouse spermatogenesis. Nat Commun 10:20. https://doi.org/10.1038/s41467-019-09182-1.
48. Zhu D, Li C, Swanson AM, Villalba RM, Guo J, Zhang Z, Matheny S, Murakami T, Stephenson JR, Daniel S, Fukata M, Hall RA, Olson JJ, Neigh GN, Smith Y, Rainnie DG, Van Meir EG. 2015. BAI1 regulates spatial learning and synaptic plasticity in the hippocampus. J Clin Invest 125:1497–1508. https://doi.org/10.1172/JCI74603.
49. Rigotti A, Trigatti BL, Penman M, Rayburn H, Herz J, Krieger M. 1997. A targeted mutation in the murine gene encoding the high density lipoprotein (HDL) receptor scavenger receptor class B type I reveals its key role in HDL metabolism. Proc Natl Acad Sci U S A 94:12610–12615. https://doi.org/10.1073/pnas.94.23.12610.
50. Lu Q, Gore M, Zhang Q, Camenisch T, Boast S, Casagranda F, Lai C, Skinner MK, Klein R, Matsushima GK, Earp HS, Goff SP, Lemke G. 1999. Tyro-3 family receptors are essential regulators of mammalian spermatogenesis. Nature 398:723–728. https://doi.org/10.1038/19554.
51. Lemke G. 24 April 2019, posting date. How macrophages deal with death. Nat Rev Immunol 36:1–11. https://doi.org/10.1038/s41577-019-0167-y.
52. Rothlin CV, Carrera-Silva EA, Bosurgi L, Ghosh S. 2015. TAM receptor signaling in immune homeostasis. Annu Rev Immunol 33:355–391. https://doi.org/10.1146/annurev-immunol-032414-112103.
53. Coultas L, Bouillet P, Loveland KL, Meachem S, Perlman H, Adams JM, Strasser A. 2005. Concomitant loss of proapoptotic BH3-only Bcl-2 antagonists Bik and Bim arrests spermatogenesis. EMBO J 24:3963–3973. https://doi.org/10.1038/sj.emboj.7600857.
54. Honarpour N, Du C, Richardson JA, Hammer RE, Wang X, Herz J. 2000. Adult Apaf-1-deficient mice exhibit male infertility. Dev Biol 218:248–258. https://doi.org/10.1006/dbio.1999.9585.
55. Kasai S, Chuma S, Motoyama N, Nakatsuji N. 2003. Haploinsufficiency of Bcl-x leads to male-specific defects in fetal germ cells: differential regulation of germ cell apoptosis between the sexes. Dev Biol 264:202–216. https://doi.org/10.1016/S0012-1606(03)00400-7.
56. Print CG, Loveland KL, Gibson L, Meehan T, Stylianou A, Wreford N, de Kretser D, Metcalf D, Köntgen F, Adams JM, Cory S. 1998. Apoptosis regulator bcl-w is essential for spermatogenesis but appears otherwise redundant. Proc Natl Acad Sci U S A 95:12424–12431. https://doi.org/10.1073/pnas.95.21.12424.
57. Rodriguez I, Ody C, Araki K, Garcia I, Vassalli P. 1997. An early and massive wave of germinal cell apoptosis is required for the development of functional spermatogenesis. EMBO J 16:2262–2270. https://doi.org/10.1093/emboj/16.9.2262.
58. Surh CD, Sprent J. 1994. T-cell apoptosis detected *in situ* during positive and negative selection in the thymus. Nature 372:100–103. https://doi.org/10.1038/372100a0.
59. Biermann M, Maueröder C, Brauner JM, Chaurio R, Janko C, Herrmann M, Muñoz LE. 2013. Surface code–biophysical signals for apoptotic cell clearance. Phys Biol 10:065007. https://doi.org/10.1088/1478-3975/10/6/065007.
60. Lee J, Richburg JH, Younkin SC, Boekelheide K. 1997. The Fas system is a key regulator of germ cell apoptosis in the testis. Endocrinology 138:2081–2088. https://doi.org/10.1210/endo.138.5.5110.
61. Rato L, Alves MG, Socorro S, Duarte AI, Cavaco JE, Oliveira PF. 2012. Metabolic regulation is important for spermatogenesis. Nat Rev Urol 9:330–338. https://doi.org/10.1038/nrurol.2012.77.
62. Xiong W, Wang H, Wu H, Chen Y, Han D. 2009. Apoptotic spermatogenic cells can be energy sources for Sertoli cells. Reproduction 137:469–479. https://doi.org/10.1530/REP-08-0343.
63. Huang J, Wang H, Chen Y, Wang X, Zhang H. 2012. Residual body removal during spermatogenesis in C. elegans requires genes that mediate cell corpse clearance. Development 139:4613–4622. https://doi.org/10.1242/dev.086769.
64. Getun IV, Torres B, Bois PRJ. 15 April 2011, posting date. Flow cytometry purification of mouse meiotic cells. JoVE https://doi.org/10.3791/2602.

65. Koh KB, Komiyama M, Toyama Y, Adachi T, Mori C. 2004. Percoll fractionation of adult mouse spermatogonia improves germ cell transplantation. Asian J Androl 6:93–98.
66. Lassalle B, Ziyyat A, Testart J, Finaz C, Lefèvre A. 1999. Flow cytometric method to isolate round spermatids from mouse testis. Hum Reprod 14:388–394. https://doi.org/10.1093/humrep/14.2.388.
67. Nomura S, Satoh M, Fujita T, Higo T, Sumida T, Ko T, Yamaguchi T, Tobita T, Naito AT, Ito M, Fujita K, Harada M, Toko H, Kobayashi Y, Ito K, Takimoto E, Akazawa H, Morita H, Aburatani H, Komuro I. 30 October 2018, posting date. Cardiomyocyte gene programs encoding morphological and functional signatures in cardiac hypertrophy and failure. Nat Commun https://doi.org/10.1038/s41467-018-06639-7.